Supporting Information for:

Insights into the Mechanism of Peptide Cyclodehydrations Achieved Through the Chemoenzymatic Generation of Amide Derivatives

Kyle L. Dunbar[1,2] and Douglas A. Mitchell[1-3]*

[1]Department of Chemistry, [2]Institute for Genomic Biology, and [3]Department of Microbiology, University of Illinois at Urbana-Champaign, Urbana, Illinois, USA.

*Corresponding author; Mitchell, Douglas (douglasm@illinois.edu), phone: 1-217-333-1345, fax: 1-217-333-0508

Table of Contents:

Supporting Methods

Figure S1: Azolines in Natural Products are Protected from Nucleophiles

Figure S2: Peptide Substrate Sequences

Figure S3: ^{18}O Labeling of BalhA1 is Dependent on Azoline Heterocycles

Figure S4: Potassium Hydrosulfide (KHS) Treatment of Unmodified BalhNC-A40T

Figure S5: MALDI-MS of the BalhX BalhCD and Thiolysis Reactions

Figure S6: Thioamide Localization on BalhX

Figure S7: Azol(in)e Localization on BCD-Treated $BalhA1_{core}$

Figure S8: McbA Processing by a non-cognate BCD Complex

Figure S9: SagX Processing by a non-cognate BCD Complex

Figure S10: Leader Peptide-Free Processing Follows Previously Established Rules

Figure S11: TOMM Dehydrogenase Alignments

Figure S12: Stability and FMN Loading of McbC-K201A and -Y202A

Figure S13: Isotope Distribution of ADP Produced During [$^{18}O_5$]-BalhA1 Modification

Figure S14: ^{18}O Enrichment of [$^{18}O_5$]-BalhA1

Figure S15: Azoline Localization on BalhA2 via ^{18}O-labeling

Figure S16: Iodoacetamide Labeling of McbA Following Treatment with McbC Variants

Figure S17: Azoline Localization on McbA Following Treatment with McbC-K201A

Figure S18: Azoline Localization on McbA Following Treatment with McbC-Y202A

Figure S19: Azoline Localization on BalhD-Treated BalhA1 via ^{18}O-labeling

Figure S20: ^{18}O-labeling of Plantazolicin

Figure S21: ^{18}O-labeling of Ulithiacyclamide

Figure S22: ^{18}O-labeling of Lissoclinamide 4

Supporting Methods

BalhX Synthesis: The synthetic peptide was ordered from GenScript (www.genscript.com) and received as a lyophilized powder (92 % purity).

Dehydrogenase Alignments. Alignments were made with Clustal Omega using the standard parameters.[1]

McbC mutagenesis. The K201A and Y202A mutants of McbC (dehydrogenase involved in microcin B17 biosynthesis) were generated via site-directed mutagenesis of a pET15b plasmid containing MBP-McbC using QuikChange as per the manufacturer's instructions.

Overexpression and purification of MBP-tagged proteins. All substrates and modification enzymes, apart from Trx-BalhA1 (see below), were overexpressed and purified as previously reported.[2]

Overexpression and purification of Trx-BalhA1. BL21(DE3-RIPL) cells were transformed with a pET32b plasmid containing Trx-BalhA1 (*E. coli* thioredoxin fusion protein that bears a *N*-terminal His-tag). Cells were grown overnight on Luria-Bertani (LB) plates with 100 µg/mL ampicillin. Single colonies were picked for starter cultures containing 100 µg/mL ampicillin and 34 µg/mL chloramphenicol and were grown at 37 °C. A 10 mL overnight culture was used to inoculate 1 L of LB containing 100 µg/mL ampicillin and 34 µg/mL chloramphenicol. Cultures were grown to an optical density at 600 nm (OD_{600}) of 0.8 before induction with 1 mM isopropyl ß-D-1-thiogalactopyranoside (IPTG) for 1.5 h at 22 °C. Subsequently, cells were harvested at 3000 × *g* for 15 min, washed with TBS (Tris buffered saline; 10 mM Tris pH 7.5, 150 mM NaCl) and stored at -20 °C for up to one week before use.

Cell pellets were resuspended in lysis buffer [50 mM Tris pH 8, 500 mM NaCl, 25 mM imidazole, 2.5% glycerol (v/v), 0.1% Triton X-100 (v/v)] containing lysozyme (4 mg/mL), leupeptin (2 µM), PMSF (200 µM), benzamidine (2 mM), and E64 (2 µM). After a 30 min incubation at 4 °C, cells were disrupted via sonication 3 × 30s with 10 min equilibration periods at 4 °C. The insoluble debris was removed from the sample via centrifugation at 20,000 × *g* for 45 min. The resulting supernatant was applied to pre-equilibrated Ni-NTA resin (Qiagen, 5 mL resin per L of cells). The column was washed with 10 column volumes of lysis buffer, followed by 5 column volumes of wash buffer (lysis buffer with NaCl concentration increased to 300 mM and Triton X-100 omitted). The His-tagged proteins were eluted using 4 column volumes of elution buffer (wash buffer with 150 mM NaCl and 200 mM imidazole) and the eluent was concentrated using an appropriate Amicon Ultra centrifugal filter (Millipore). A 100-fold buffer exchange with storage buffer [50 mM HEPES pH 7.5, 150 mM NaCl, 2.5% glycerol (v/v)] was performed in the filtration device before a final concentration and storage. After loading onto the column, all buffers used contained 1 mM tris-(2-carboxylethyl)-phosphine (TCEP). Protein concentration was determined both by the 280 nm absorbance and a Bradford colorimetric assay (Thermo Scientific). Purity was visually assessed by Coomassie-stained SDS-PAGE gel.

^{18}O labeling of BalhA2, BalhD-treated BalhA1, and McbC-K201A/Y202A reactions. 100 μM MBP-BalhA2 was incubated with 1 μM MBP-BalhC/D in synthetase buffer for 18 h at 25 °C. The resultant tetra-azoline peptide was trypsin digested with 0.02 mg/mL trypsin (sequence grade, Promega) for 2 h at 25 °C before being lyophilized to dryness to remove all [^{16}O]-H_2O. The resultant solid was reconstituted with ½ of the initial volume of 97 atom % [^{18}O]-H_2O and 10% formic acid in [^{16}O]-H_2O (v/v) was added to a final concentration of 0.5% (v/v). This resulted in a final isotopic enrichment of approximately 92 atom %. Azoline hydrolysis was allowed to proceed for 18 h at 25 °C. Following hydrolysis, the localization of the ^{18}O labels was carried according to Fourier-transform MS/MS procedure listed in the main text.

In the case of the McbC-K201A and -Y202A reactions, 20 μM MBP-McbA was incubated with 1 μM MBP-tagged McbB/D and either K201A or Y202A McbC in synthetase buffer for 18 h at 25 °C. Reactions were then initiated by the addition of 0.02 μg/mL thrombin (from bovine plasma) to remove the MBP tags. Unlike the Balh cyclodehydratase, the Mcb synthetase requires the removal of MBP to be catalytically active. Processing of McbA with concurrent thrombin cleavage was allowed to proceed for 18 h at 25 °C. Following cyclization, the sample was handled as described above.

For the cyclization of BalhA1 by BalhD, 25 μM BalhD and 50 μM BalhA1 (both fused to MBP) were incubated with 0.2 μg/mL TEV protease in synthetase buffer for 18 h at 25 °C. Following treatment, BalhD, MBP and TEV were precipitated from the sample by the addition of acetonitrile to a final concentration of 50% (v/v). The precipitated proteins were removed from the sample by centrifugation at 15,000 × g and the supernatant was dried on a SpeedVac (Savant, Thermo Scientific). The resultant solid was resuspended in [^{18}O]-H_2O and isotope labeling, trypsin digestion, and FT-MS/MS sequencing was carried out as described above.

ADP isotope composition. A portion (1 μL) of the of the Trx-$^{18}O_5$-BalhA1 sampled prepared for ^{31}P-NMR analysis was reserved for MALDI-MS. This sample was spotted onto the MALDI target and overlaid with 1 μL of a saturated solution of 9-aminoacridine in 50% aqueous acetonitrile. As a control, 1 mM ADP in ATP-free synthetase buffer was spotted in an analogous fashion. Both samples were analyzed on a Bruker Daltonics UltrafleXtreme MALDI-TOF in negative reflector mode.

ATP/azole stoichiometry following azoline hydrolysis. An azoline hydrolysis reaction was carried out on Trx-BalhA1 in an identical fashion to the ^{31}P-NMR experiment (see methods in main text) except [^{16}O]-H_2O was used in place of [^{18}O]-H_2O. Following buffer exchange to remove ADP and inorganic phosphate (P_i), a reaction was carried out with 50 μM BalhA1 and 2 μM BCD in low-salt synthetase buffer (50 mM Tris pH 8.5, 25 mM NaCl, 5 mM $MgCl_2$, 10 mM DTT, and 2 mM ATP) for 3 h at 25 °C. The sample was then divided into two aliquots and frozen in liquid nitrogen. The samples were analyzed by LCMS (to detect azole heterocycles) and a malachite green assay (to detect P_i).

LCMS detection of ring formation. Heterocycle content was determined as previously reported.[2]

Malachite green phosphate detection assay. P_i quantification was conducted with slight modifications to a previously described method.[2] For determining the stoichiometry of azoline formation to ATP consumption, samples were diluted 1:10 in water to a final volume of 80 µL to remove any background signal from unreacted ATP. This solution was transferred to a 96-well plate where the reaction was initiated by the addition of 20 µL malachite green working reagent (BioAssay Systems). Reactions were allowed to develop for 20 min before the absorbance was recorded at 620 nm. A standard curve was made from a known concentration of P_i in appropriately diluted synthetase buffer. The absorbance for each sample was corrected for any background originating from the buffer. Alternatively, the level of contaminating P_i in the buffer exchanged Trx-[$^{18}O_5$]-BalhA1 sample was determined by conducting the malachite green assay with 80 µL of undiluted sample. In both cases the analysis of all samples was performed in triplicate.

MS/MS localization thioamides and azol(in)e heterocycles. To locate the thioamide on BalhX and the heterocyclized sites of $BalhA1_{core}$, ion trap (IT)-MS/MS was used instead of FT-MS/MS. In both cases, samples were directly infused onto a Thermo Fisher Scientific LTQ-FT hybrid linear ion trap operating at 11 T using an Advion Nanomate 100. A full FTMS scan was conducted on all samples followed by IT-MS/MS of selected ions. FTMS scan parameters: minimal target signal counts: 5,000; resolution: 100,000; *m/z* range: variable. IT-MS/MS parameters: minimum target signal counts: 5,000; *m/z* range: dependent on target *m/z*; isolation width: 5 *m/z*; normalized collision energy: 35; activation q value: 0.25; activation time: 30 ms. Data analysis was conducted using the Qualbrowser application of Xcalibur v 2.2 (Thermo Fisher Scientific).

Iodoacetamide labeling of McbA in McbC-K201A and -Y202A reactions. Reactions were carried out with 20 µM MBP-McbA, 1 µM MBP-McbB/D (cyclodehydratase), and 1 µM of either WT, K201A or Y202A McbC (dehydrogenase) in synthetase buffer. A reaction lacking McbC was also performed as a control. MBP tag removal was performed concurrently with cyclodehydration by the addition of 0.02 µg/mL thrombin (from bovine plasma). Following an 18 h reaction at 25 °C, the samples were C_{18} ZipTip (Millipore) purified according to the manufacturer's instructions and eluted into 50% acetonitrile in 10 mM MOPS pH 8.0 with 50 mM iodoacetamide. Labeling proceeded at 25 °C for 8 h before analysis on a Bruker Daltonics UltrafleXtreme MALDI-TOF in positive reflector mode with α-cyano-hydroxycinnamic acid (CHCA) as the matrix.

^{18}O-labeling of TOMM natural products. Purified samples of plantazolicin, ulithiacyclamide and lissoclinamide 4 were dissolved in [^{18}O]-H_2O to a final concentration of 250 µg/mL and each sample was acidified via the addition of 1% formic acid. Azoline hydrolysis was allowed to proceed for 40 h at 25 °C before the samples were ZipTip desalted and analyzed on a Bruker Daltonics UltrafleXtreme MALDI-TOF as described above.

Figure S1. Azolines in natural products are protected from nucleophiles. Select azoline containing natural products are displayed with thiazolines and (methyl)oxazolines colored red. The class of natural product to which the compound belongs along with the known bioactivity of the compound is listed under each structure. In each instance, the azoline heterocycles are either sterically (*e.g.* ulithiacyclamide, yersiniabactin) or electronically (*e.g.* plantazolicin, telomestatin) protected from nucleophilic attack. RiPP, ribosomally synthesized posttranslationally modified peptide; NRP, nonribosomal peptide.

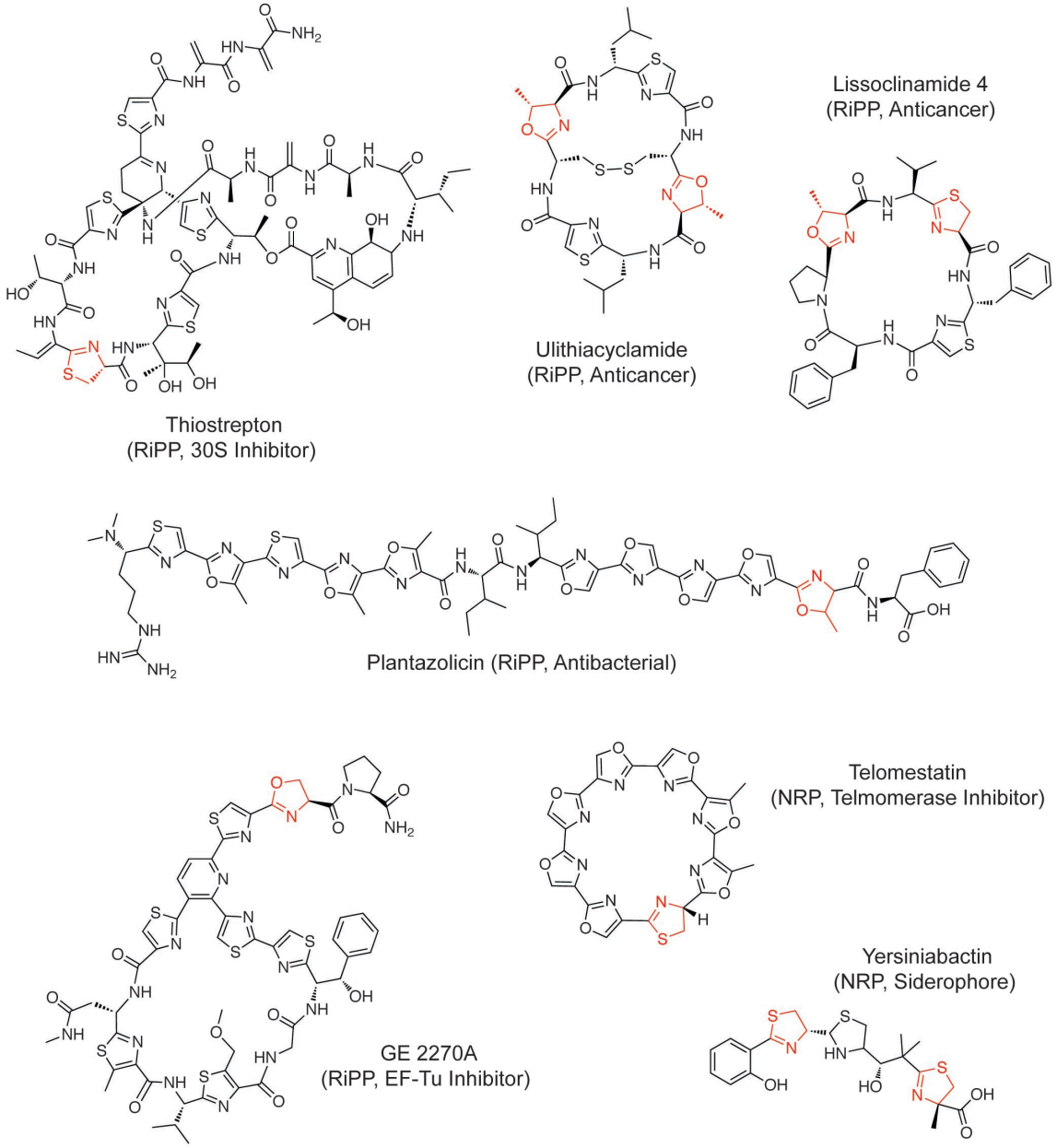

Figure S2. Peptide substrate sequences. The substrates used in this paper are listed below. Known heterocyclization sites are highlighted in red, with the exception of the first bisheterocycle site in McbA, which is highlighted in orange. In McbA, the red underlined serine is the site of the ninth heterocycle that is installed *in vitro* and found as a minor species during the microcin B17 heterologous expression.[3] The predicted site of the azoline heterocycle in BalhA2 from our previous studies is colored blue.[4] Putative and known leader peptide cleavage sites are marked with a caret and an asterisk, respectively. As SagX is an unnatural TOMM analog (see reference [5] for description), no residues are colored.

BalhA1	MEQKKILDIKLTETGKINYAHKPDD^SGCAGCMGCAGGTGCAGTGCIGQGVWKKCSGK
BalhNC-A40C	MEQKKILDIKLTETGKINYAHKPDD^AGAAGAMGAAGGVGCAGVGAIGQGVWKKAAGK
BalhNC-A40T	MEQKKILDIKLTETGKINYAHKPDD^AGAAGAMGAAGGVGTAGVGAIGQGVWKKAAGK
$BalhA1_{core}$	SGCAGCMGCAGGTGCAGTGCIGQGVWKKCSGK
BalhX	KGAAGGVGTAGVGAIGK
BalhA2	MEQKKSLDIKLTESGKIDYAHKPDD^SGCAACIGTTSCGGVDPTKPGIWKRCSSK
McbA	MELKASEFGVVLSVDALKLSRQSPLG*VGIGGGGGGGGGGSCGGQGGGCGGCSNGCSGGNGGSGGSGSHI
SagX	MLKFTSNILATSVAETTQVAPGG^CCCCGGIAGAINGGSGGSYTPNK

Figure S3. ^{18}O labeling of BalhA1 is dependent on azoline heterocycles. To ensure that the installation of ^{18}O-labels into BalhA1 was dependent on the presence of azoline heterocycles, both unmodified (1) and the penta-azole (2) forms of BalhA1 were treated with 0.5% formic acid in [^{18}O]-H_2O for 18 h. The resultant MALDI-TOF mass spectra demonstrated that in both cases, the peptides were insensitive to the ^{18}O exchange conditions. These data suggested that this strategy for substrate labeling would be selective for azoline-containing peptides. All listed masses are for the 1+ charge state. The filled circle represents an ^{18}O label.

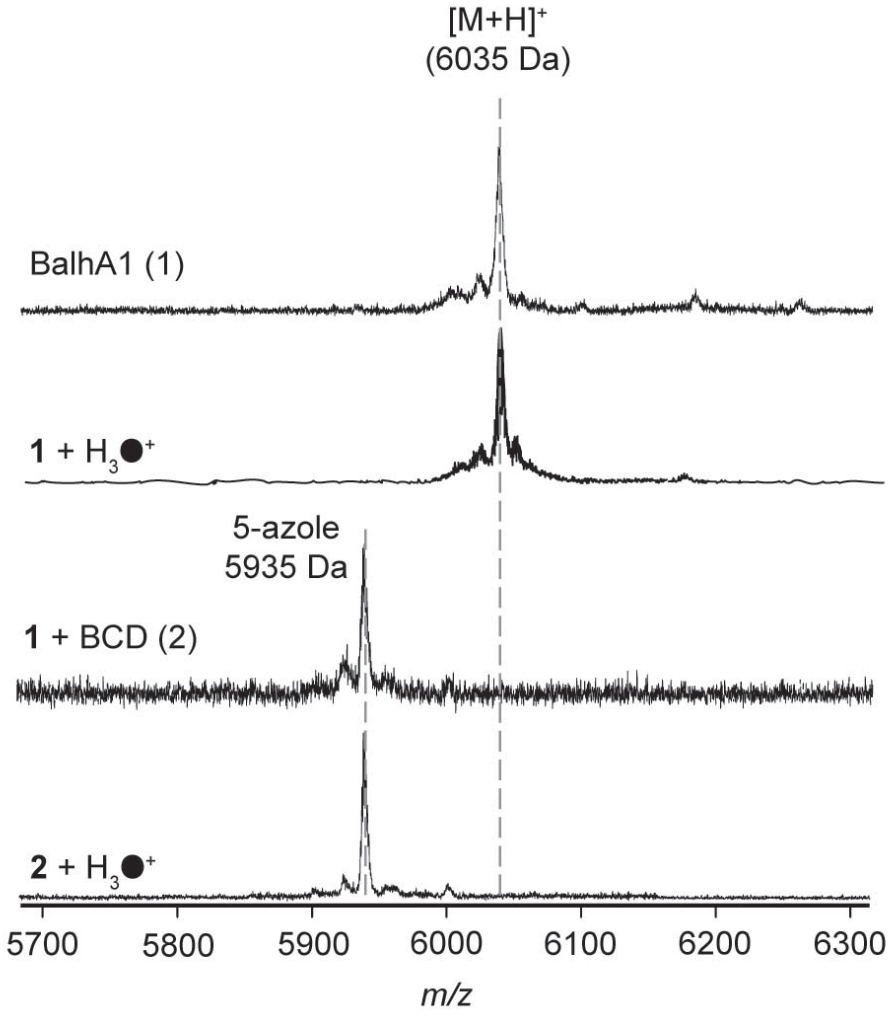

Figure S4. Potassium hydrosulfide (KHS) treatment of unmodified BalhNC-A40T. To ensure that the thiolysis of BalhNC-A40T is dependent on the presence of azoline heterocycles, unmodified substrate was treated with 100 mM KHS for 18 h at 25 °C. The resultant MALDI-TOF spectra demonstrate that the peptide is insensitive to the thiolysis conditions. These data suggest that this strategy for thioamide formation will be selective for azoline-containing peptides. All listed masses are for the 1+ charge state.

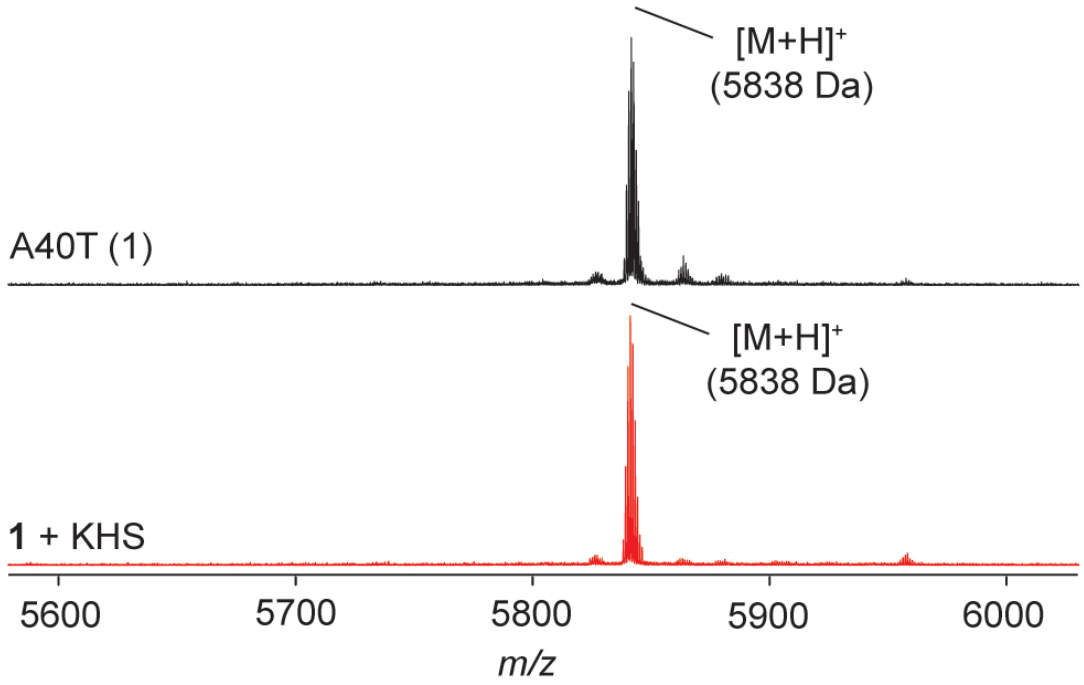

Figure S5. MALDI-MS of the BalhX BalhCD and thiolysis reactions. A MALDI-TOF spectrum of BalhCD-treated BalhX (a substrate lacking a leader peptide, Figure S2) is shown below. BalhX is derived from the core pThe spectra show that upon treatment with BalhCD, the single cyclizable residue is converted to an azoline heterocycle. Following azoline formation, BalhX was subjected to KHS treatment. The last spectrum shows that the methyloxazoline on BalhX is converted to a thioamide. The masses correspond to the 1+ charge state of the peptide and the mass shifts relative to the unmodified peptide are displayed under each label.

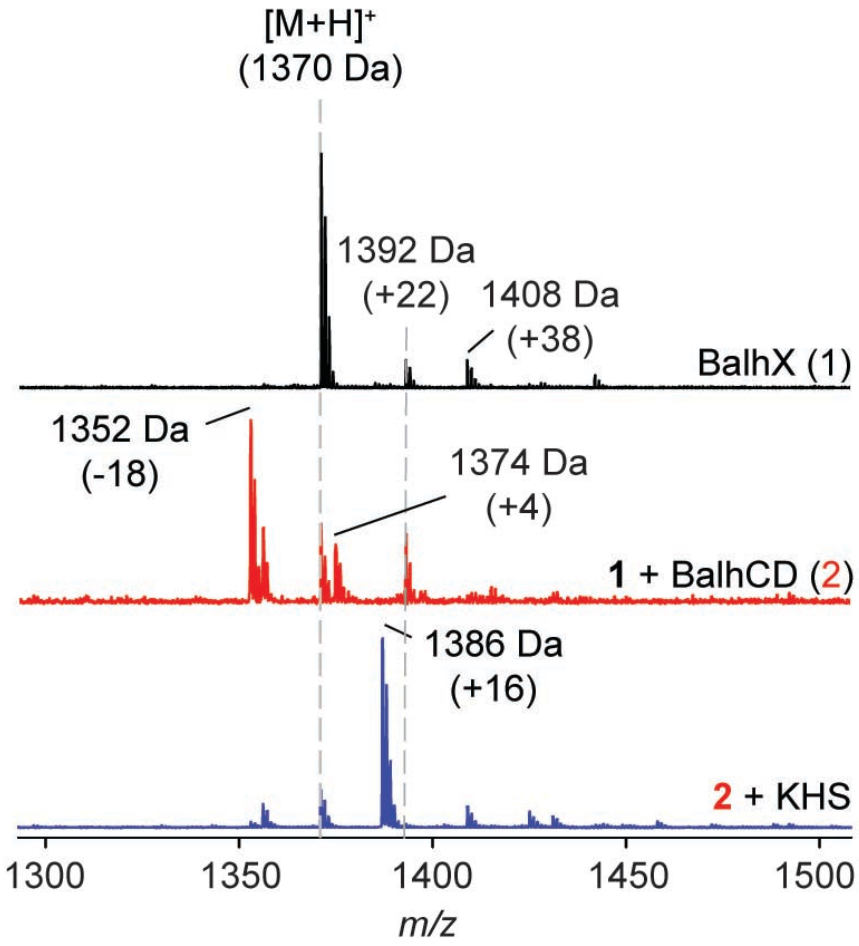

Figure S6. Thioamide localization on BalhX. An ion trap-MS/MS spectrum of the BalhX peptide following thiolysis is displayed below. The b and y ions along with the corresponding b and y ion symbols are colored based on the presence of the sulfur atom (+16 Da) in the fragment (red, contains the sulfur; black, does not). Based on the fragmentation, it is possible to definitively localize the thioamide moiety to the Gly (red) immediately upstream of the Thr that was cyclized in the starting material.

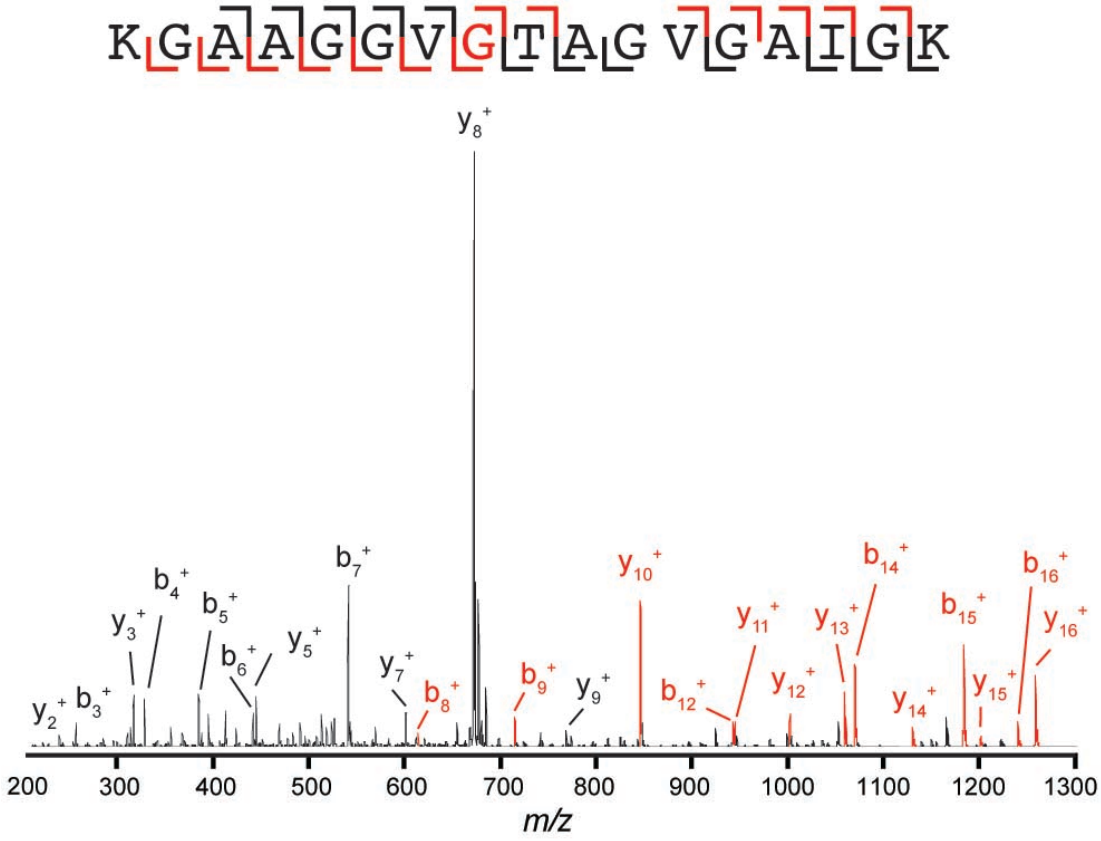

Figure S7. Azol(in)e localization on BCD-treated BalhA1$_{core}$. **(a)** An FT-MS spectrum of BCD-treated BalhA1$_{core}$ is displayed. The calculated and observed masses for the tetra-azole, mono-azoline form of the peptide in the 4+ charge state are shown along with the ppm error of the measurement. **(b)** An FT-MS/MS spectrum of the species shown in panel **(a)**. The b and y ions are colored based on the number of heterocycles found in the fragment (green, 5; purple, 4; orange, 3; blue, 2; red, 1; black, 0). Asterisks denote ions with a neutral loss of water. The yellow stars denote the sites of azole formation while the blue star denotes the lone azoline site. This data shows that the same positions in the BalhA1 core peptide are modified when the leader peptide is removed, and that the azoline oxidation is dysregulated on substrates lacking a leader peptide.

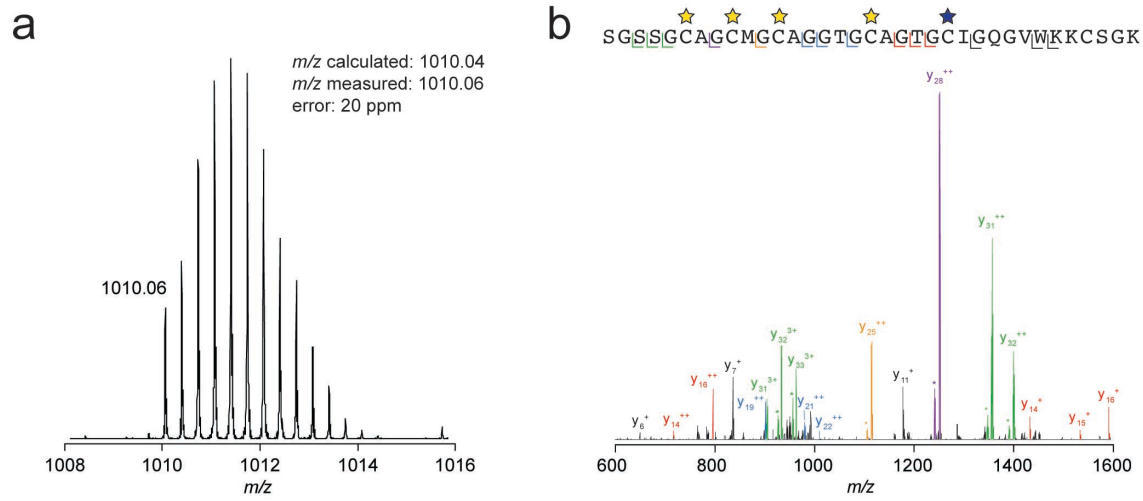

Figure S8. McbA processing by a non-cognate BCD complex. A MALDI spectrum of BcerB/BalhCD-treated McbA is shown. All displayed masses are for the 1+ charge state. The mass shift relative to the unmodified species is shown below the mass of the peak in the BCD-treated sample. This spectral overlay demonstrates that the Balh synthetase was able to modify a non-cognate substrate irrespective of the presence of a Balh leader peptide. However, the efficiency of modification was decreased relative to a McbA core peptide fused to the BalhA1 leader peptide as the chimera substrate was primarily converted to a tri-azole form under analogous reaction conditions.[4]

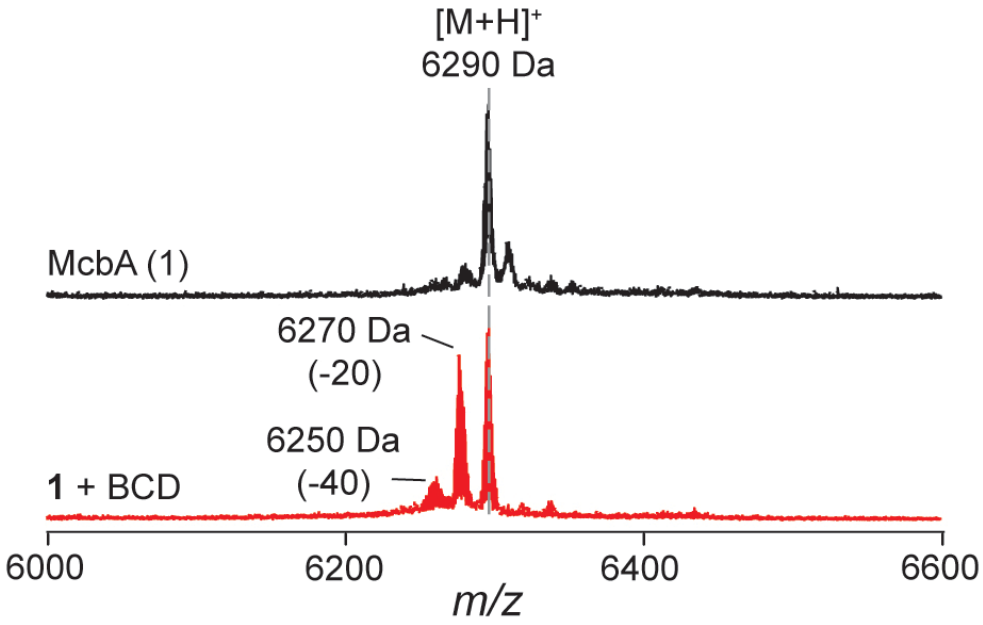

Figure S9. SagX processing by a non-cognate BCD complex. A MALDI spectrum of BcerB/BalhCD-treated SagX is shown. SagX is an unnatural derivative of SagA (the streptolysin S precursor peptide) comprised of the SagA leader peptide and an unnatural core domain.[5] All displayed masses are for the 1+ charge state. The mass shift relative to the unmodified species is shown below the mass of the peak in the BCD treated sample. The spectra demonstrate that two heterocycles, one azole and one azoline, are installed in SagX by the Balh synthetase complex.

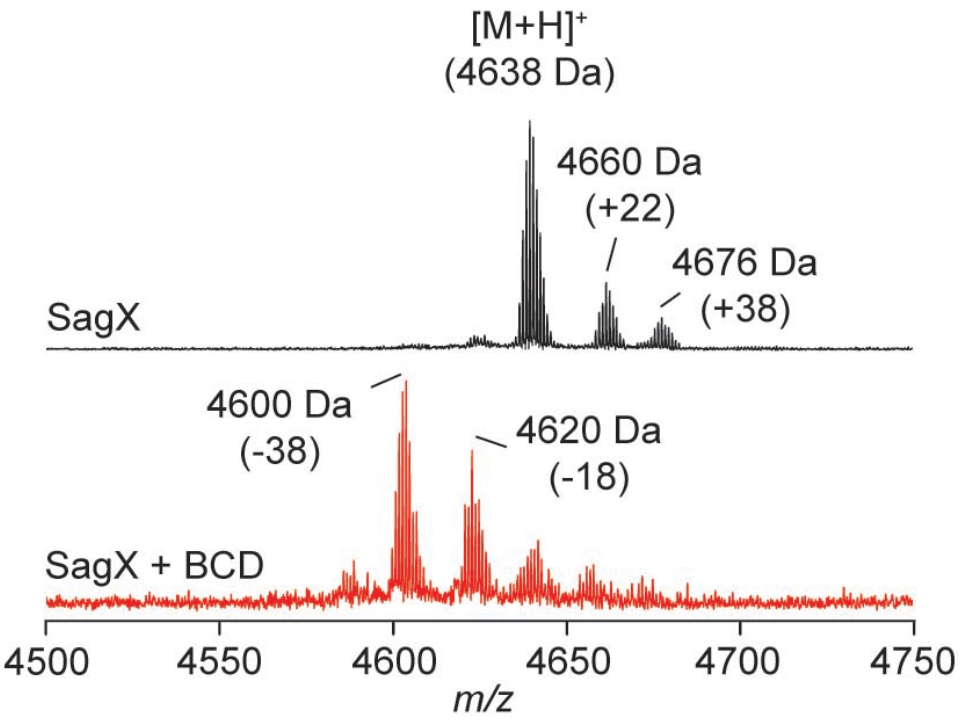

Figure S10. Leader peptide-free processing follows previously established rules. While the Balh cyclodehydratase was able to modify McbA (Figure S8), SagX (Figure S9) and BalhX (Figure S5), each of these unnatural leader peptide-free substrates contained an optimal cyclization sequence: Gly in -1; non-proline in +1 (Figure S2). (**a**) Three peptides lacking this optimal heterocyclization sequence are displayed with heterocyclizable residues colored blue. In order to determine if these selection rules still applied in leader peptide-free substrates the three peptides shown in panel (**a**) were treated with BalhCD overnight. (**b**) The MALDI-TOF spectra of the BalhCD-treated peptides are shown. In all cases, treatment with the Balh cyclodehydratase failed to result in substrate processing, even at substrate:enzyme ratios of 1:1. Apart from the terminal Ser on ClosA-LP, all of the heterocyclizable residues are downstream of a non-Gly residue and are not processed. The C-terminal Ser on ClosA-LP is likely not processed due to the lack of a +1 residue. When viewed together with McbA, SagX, BalhX and $A1_{core}$ processing, these data suggest that the selectivity of the Balh cyclodehydratase has been retained when the leader peptide is not present. All masses correspond to the 1+ charge state.

a

SagA-LP MLKFTSNILATSVAETTQVAPGG
ClosA-LP MLKFNEHVLTTTNNSNNKVTVAPGS
PznA MEEATIMTQIKVPTALIASVHGEGQHLFEPMAARCTCTTIISSSSTF

b

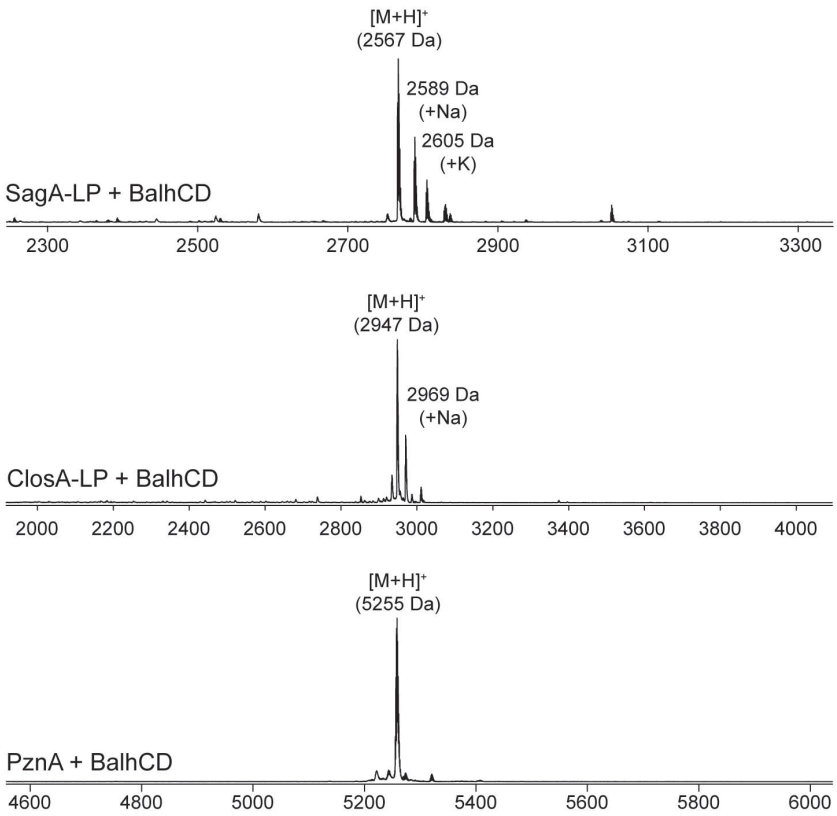

Figure S11. TOMM dehydrogenase alignments. A Clustal Omega alignment of dehydrogenases from diverse TOMM clusters is displayed (for a larger alignment see reference [6]). Residues predicted to be involved in coordinating the phosphate moiety of FMN (based on the crystal structure of a non-TOMM "nitroreductase", PDB entry 3EO7) are colored blue. The residues highlighted in red were chosen for the mutagenesis due to their high level of conservation and the prediction that they were not directly involved in FMN binding. In McbC, these residues are K201 and Y202.

```
BcerB          LNNRKSVEE-----------LEIRTRIRFETLSNLLHFSYGYINKP-------------H
ClosB          IKSRRSVRR-----------YSS-KSMSLNDVANIFYYTQGICDEVEPYNLEGNKKKIKL
McbC           VINISSSHNFSRERLPSGINFCDKNKLSIRTIEKLLVNAF-----------SSPDPGSVR
LlsB           LEQRHSTRN-----------FVY-ETMDLSTFSNIIQFSFGLSTRKLVYN----DLQSTT
PagB           IVTRRSIRT-----------FSY-EPIKLNELSVLLKLSSGVVLIQDE-----ENHSIYH
PatG           IETRQSIRE-----------YDD-YPITIEQLGELLYRCARVTEVY----QMEEVGEVSR
PznB           IQNRRSIEQ-----------FNG-GSTTLAQLSTILQGSYGLIERP----------EGPR
SagB           IIKRRSHRQ-----------FSD-RQMPLQDLSNILYYACGVSSQAS--IRDGASDKITL
               :    * .                    :  .  ::

BcerB          SAAPSAGGKYPINIYIAVFN--VENL--EQGIYYYDREQDVLDMIRRGD----------F
ClosB          RANPSAGGLYPIELYVYMKS--IKDL--EDGIYTYYPYSHGLKPIKVNKEALKIENFAEF
McbC           RPYPSGGALYPIEVFLCRLSENTENWQAGTNVYHYLPLSQALEPVATCNTQSLYRSLSG-
LlsB           RHYSSGGGLYPIDVFLYINN--ISGI--AKGIYKYQPYTHSLHPLDVDK--IDVESFFVG
PagB           RSFPTAGGLNSCHVYLISLN--VDDL--PFGSYYYDPLTHELIKIEEYQI----SQKNEF
PatG           RPYPCGGARYELEIYPVVQQ--CEGL--DAGLYHYDPLNHQLEQIADYNPEVAA-----L
PznB           RPIPSGGALYPLDLYVVSNK--VDSL--EKGLYHFDPYRKGLVHLGEYSE----EDFGR-
SagB           RNCASGGGLYPIHLVFYARN--ISKL--IDGFYEYLPYQHALRCYRHSS-EENVRDFAEY
                    .*.    .:     .   .        * :    . *      .

BcerB          RESINNLYVDNTHIHSSSFIMFHAANLDQTSSKYADRGYKLIHLDMGHLSQNLYLLSSAQ
ClosB          ---------GVLNAENANLIVFYVYNFLKNSRKYGDAGFSYALIETGEMAQNLQLVSTAL
McbC           --------GDSERLGKPHFALVYCIIFEKALFKYRYRGYRMALMETGSMYQNAVLVADQI
LlsB           ---------DNIDTSNMNFCVFFGYSINKNYVKYGELSLLNTFVELGGISHNFDLVCHSV
PagB           LDTLVKVLGNQEWIRTAGLILIITGDYSKIRLKYGDRGYRYLLLEAGHIMQNFYLIASML
PatG           ---IADARLSSGEQDTPQVLLIITARFGRLFCKYKSLAYALVLKHVGVLYENLYLVATDM
PznB           ------IMLQEEAVKDFSFAVIISASFWRSRFKYGHRSYRFIFIEAGHLMQNMILLATAQ
SagB           ---------GAINAENCNIIIIYVYHYIKNTRKYGNQATAYAFIESGEIAQNIQLTATAL
                              . :.      :   **   .      . * : .*  * .
```

Figure S12. Stability and FMN loading of McbC-K201A and -Y202A. **(a)** An Coomassie-stained SDS-PAGE gel of amylose resin purified WT, K201A, and Y202A MBP-McbC is displayed along with a table listing the yield of each protein. While the Y202A mutant was lower yielding, the SDS-PAGE gel indicated that the protein was not structurally destabilized to any significant extent, as would be evidenced by faster migrating proteolytic degradation bands. **(b)** In order to determine the effect, if any, the K201A and Y202A mutations had on FMN-binding in McbC, a UV-vis absorbance spectrum was acquired for each protein. The ratio of the absorbance at 450 and 280 nm was used to evaluate FMN-loading. While Y202A has a slightly lower molar absorptivity at 280 nm than WT McbC, the difference is less than 2% and within the error of the measurement. The graph shows the loading for each of the mutants has not been drastically effected by the mutations, relative to WT McbC. Error bars represent the standard deviation from the mean (n = 3).

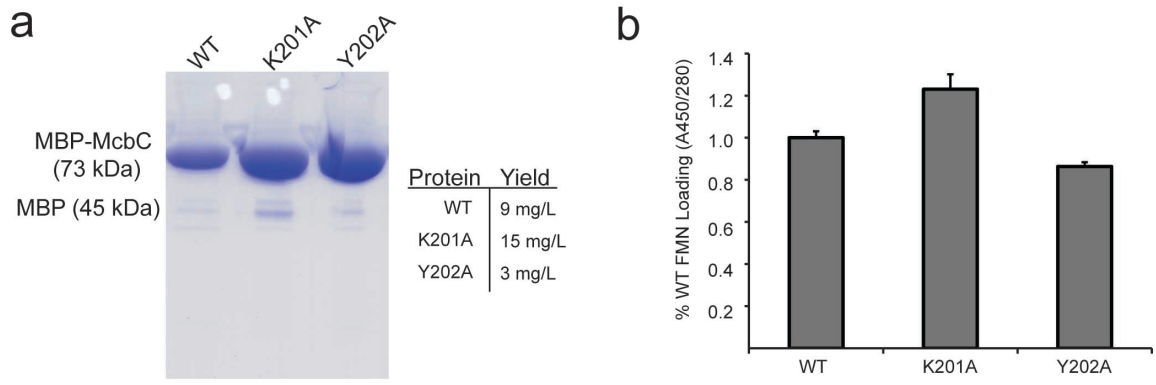

Figure S13. Isotope distribution of ADP produced during [$^{18}O_5$]-BalhA1 modification. A negative mode MALDI-TOF spectral overlay of an ADP standard (black) and the ADP produced during ^{18}O-BalhA1 (red) processing is shown. If [$^{16}O_4$]-P_i production is due to ^{18}O incorporation into ADP, the second isotope peak of ADP should be approximately the same height of the monoisotopic peak; however the isotope distribution of ADP produced in the Trx-[$^{18}O_5$]-BalhA1 reaction is unperturbed relative to an ADP standard. This data demonstrates that isotope scrambling is not the cause of the [$^{16}O_4$]-P_i peak in the ^{31}P-NMR sample (also see Figure 3 of the main text).

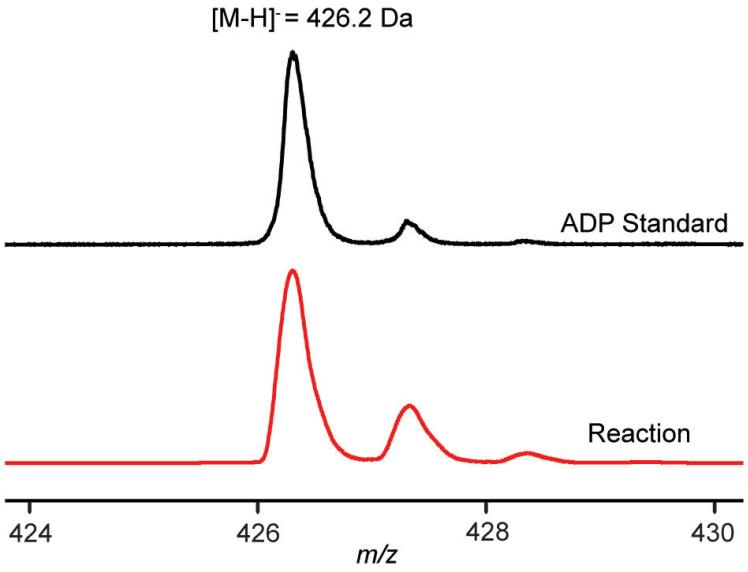

Figure S14. ^{18}O enrichment of [$^{18}O_5$]-BalhA1. A high-resolution mass spectrum of [$^{18}O_5$]-BalhA1 is displayed below. The peaks are colored according to the number of ^{18}O labels in the peptide (green, five; purple, 4; orange, 3; blue, 2; red, 1; black, 0). The calculated and measured masses of the [$^{18}O_5$]-BalhA1 peak are displayed in the 3+ charge state along with the ppm error of the measurement. The level of ^{18}O enrichment was determined based on the intensities of the monoisotopic peaks for each of the ^{18}O-labeled BalhA1 derivatives. The theoretical maximum ^{18}O enrichment of 92% was determined based on the final atom % of ^{18}O during the hydrolysis reaction. When this enrichment is combined with the measured ATP/ring stoichiometry for hydrolyzed peptide (see main text), an expected [$^{16}O_4$]-P_i:[$^{16}O_3{}^{18}O$]-P_i ratio of ~1.3 is obtained. This value is in good agreement with that found in the ^{31}P-NMR experiment of 1.3 (see Figure 3).

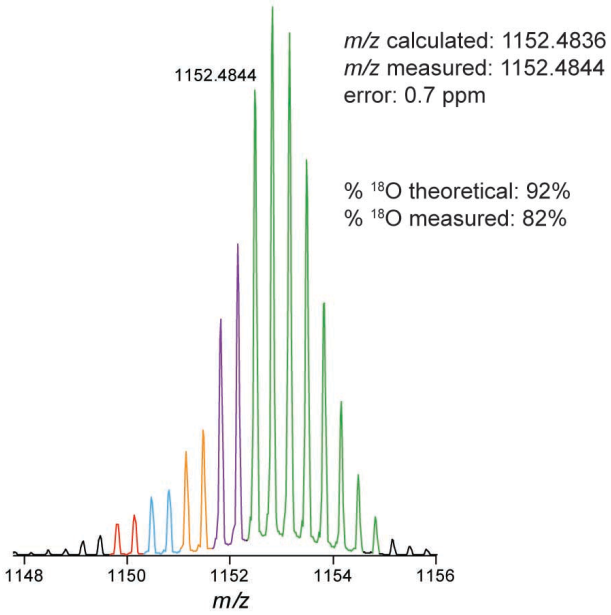

Figure S15. Azoline localization on BalhA2 via ^{18}O labeling. Following treatment with BalhCD and ^{18}O-hydrolysis, BalhA2 was subjected to FT-MS/MS. **(a)** An intact mass spectrum for [$^{18}O_4$]-BalhA2 in the 4+ charge state is displayed. The monoisotopic masses for the most prominent ^{18}O-labeled species are displayed and colored based on the number of ^{18}O labels (purple, 4; orange, 3; blue, 2). Note that the isotope distribution of the [$^{18}O_4$]-peak is skewed to higher m/z values, indicating that a [$^{18}O_5$]-labeled species also exists. The ppm error for the major species is displayed. **(b)** A MS/MS spectra of the [$^{18}O_4$]-BalhA2 species from panel **(a)** demonstrates that the oxazoline site is the first Thr, as was previously hypothesized.[4] The b and y ions are colored based on the number of ^{18}O present in the fragment (purple, 4; orange, 3; blue, 2; red, 1; black, 0). Stars represent the sites of ^{18}O labels from hydrolysis of the azoline heterocycles and asterisks label peaks with neutral water loss. Based on the y ion series, the *C*-terminal carboxylate bears a single ^{18}O label (denoted by red residue). This is a consequence of the sample preparation and is a known reaction occurring on acidified tryptic peptides.[7]

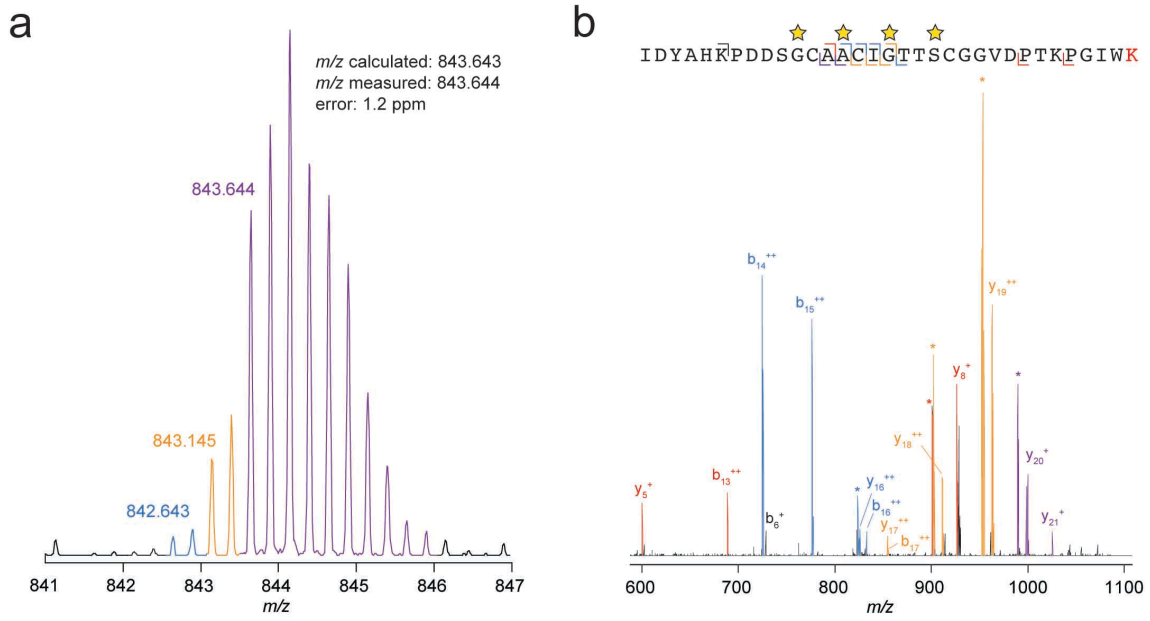

Figure S16. Iodoacetamide labeling of McbA following treatment with McbC variants. To determine if the azolines installed on McbA following treatment with McbBD and mutants of McbC were thiazolines or oxazolines, the products were subjected to iodoacetamide (IA) labeling. In the case of unmodified McbA (McbA + McbBD, top spectrum), up to five IA labels were installed. As McbA contains four Cys residues (see Figure S2), the presence of a low intensity peak corresponding to a substrate with five IA labels is likely due to the IA-dependent labeling of amines. Upon treatment with the all wild-type McbBCD (WT) complex, the peptide is no longer reactive towards IA, as all cysteines have been converted to thiazoles (Thz). In contrast, for samples treated with McbBD and either McbC-K201A or -Y202A, the di-azoline substrate undergoes two labeling events. As with the unclyclized McbA sample, both the WT and K201A/Y202A treated peptides have a low intensity peak corresponding to the non-specific IA-labeling of amines. Masses correspond to the 1+ charge state of the species and the number of IA labels, and Thz, oxazole (Oxz) and thiazoline (ThH) heterocycles are displayed beneath each mass.

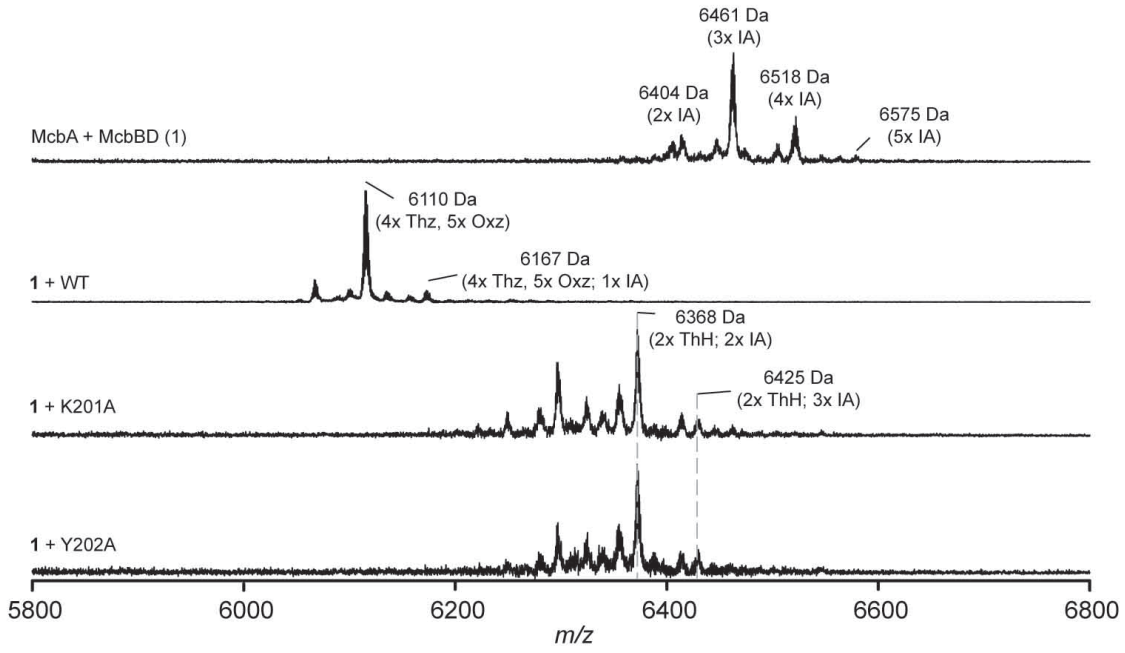

Figure S17. Azoline localization on McbA following treatment with McbC-K201A. Azoline heterocycles on McbA were subjected to ^{18}O hydrolysis to form [$^{18}O_2$]-McbA, and the labeled peptide was analyzed by FT-MS/MS to locate the sites of azoline formation. The b and y ions are colored based on the number of ^{18}O present in the fragment (blue, 2; red, 1; black, 0). Asterisks indicate peaks with a neutral loss of water. Based on the fragmentation pattern and the iodoacetamide labeling data (Figure S16), one of the thiazoline heterocycles can be definitively localized to Cys41 (red). The other thiazoline is formed at either Cys48 or Cys51 (blue). Incomplete fragmentation in this region precluded the precise localization of the modification site.

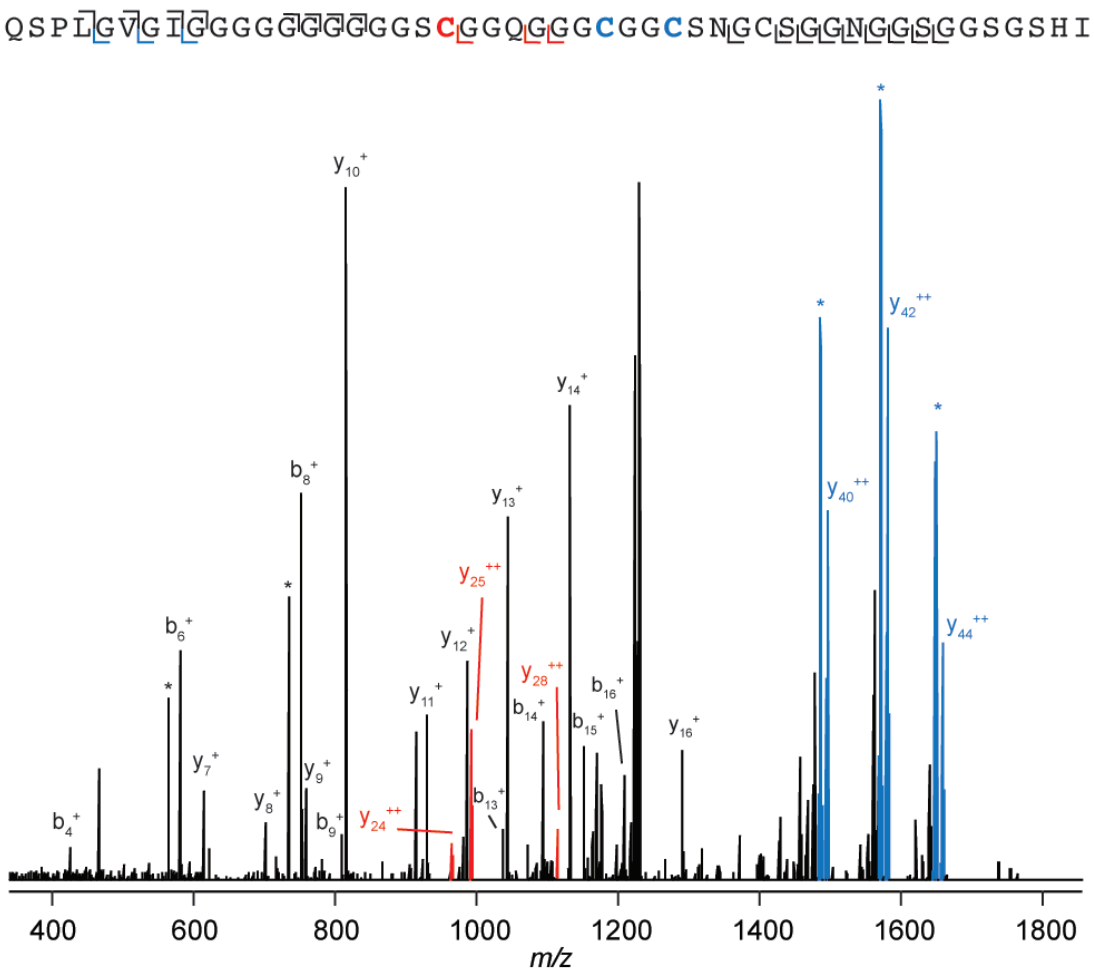

Figure S18. Azoline localization on McbA following treatment with McbC-Y201A. Azoline heterocycles on McbA were subjected to ^{18}O hydrolysis to form [$^{18}O_2$]-McbA, and the labeled peptide was analyzed by FT-MS/MS to locate the sites of azoline formation. The b and y ions are colored based on the number of ^{18}O present in the fragment (blue, 2; red, 1; black, 0). Asterisks indicate peaks with a neutral loss of water. Based on the fragmentation pattern and the iodoacetamide labeling data (Figure S12), one of the thiazoline heterocycles can be definitively localized to Cys41 (red). The other thiazoline is formed at either Cys48 or Cys51 (blue). Incomplete fragmentation in this region precluded the precise localization of the modification site.

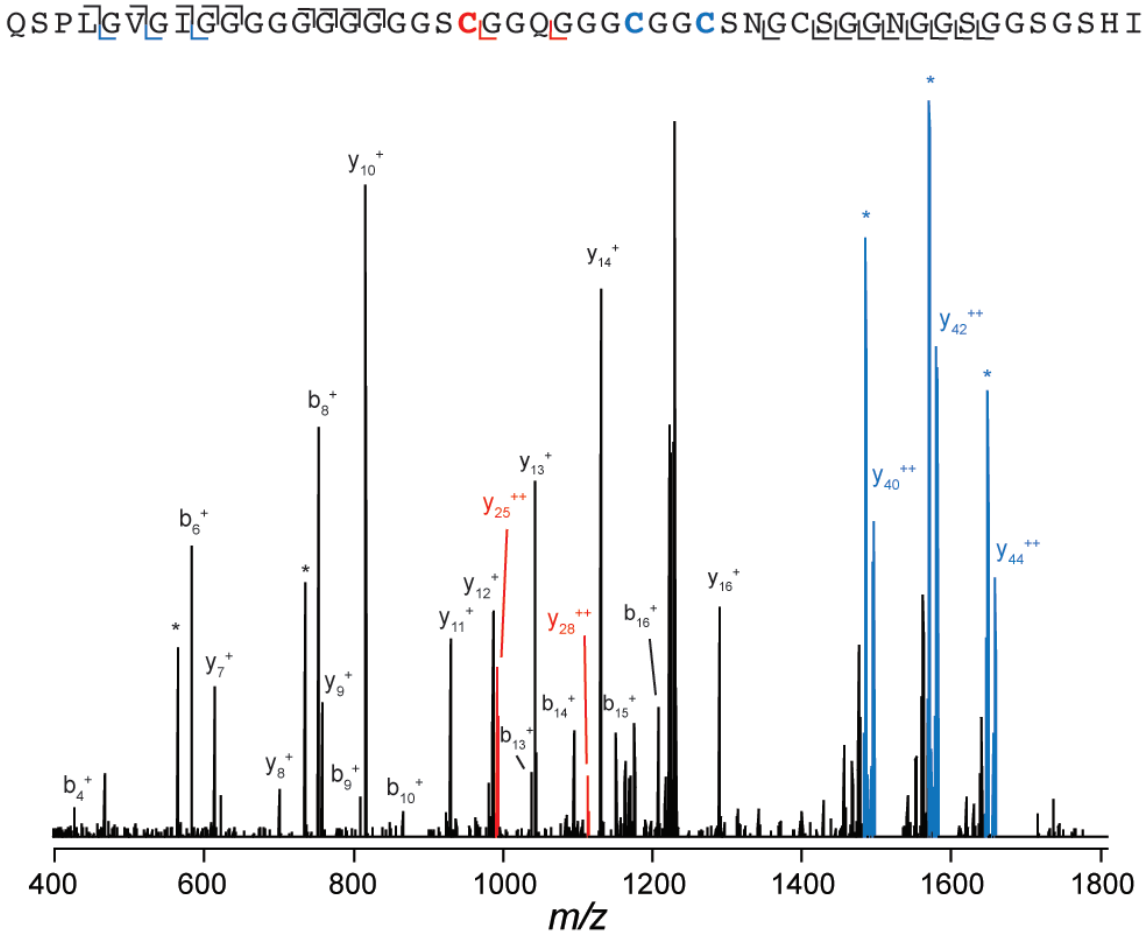

Figure S19. Azoline localization on BalhD-treated BalhA1 via ^{18}O-labeling. Following treatment with BalhD and ^{18}O-hydrolysis, BalhA1 was subjected to FT-MS/MS. **(a)** An intact mass spectrum for [$^{18}O_3$]-BalhA1 in the 4+ charge is displayed. The monoisotopic masses for the most prominent ^{18}O-labeled species are given and colored based on the number of ^{18}O labels (orange, 3; blue, 2; red, 1; black, 0). Prior to hydrolysis the peptide had two azoline heterocycles. The presence of a third ^{18}O label indicates that a non-specific labeling event occurred. The ppm error for the major species is displayed. **(b)** A MS/MS spectra of the [$^{18}O_3$]-BalhA1 species from panel **(a)** demonstrates that the two azolines are spread across three sites: Thr38, Cys40 and Cys45. Based on the b and y ion intensities, Cys45 was always found as a thiazoline, while azoline formation at Thr38 and Cys40 occurred in equal amounts. The b and y ions are colored based on the number of ^{18}O present in the fragment (orange, 3; blue, 2; red, 1; black, 0). Stars represent the sites of ^{18}O labels from hydrolysis of the azoline heterocycles and asterisks label peaks with neutral water loss. As with the BalhA2 sample (Figure S15), the y ion series indicates that the *C*-terminal carboxylate has a single ^{18}O label (denoted by red residue).

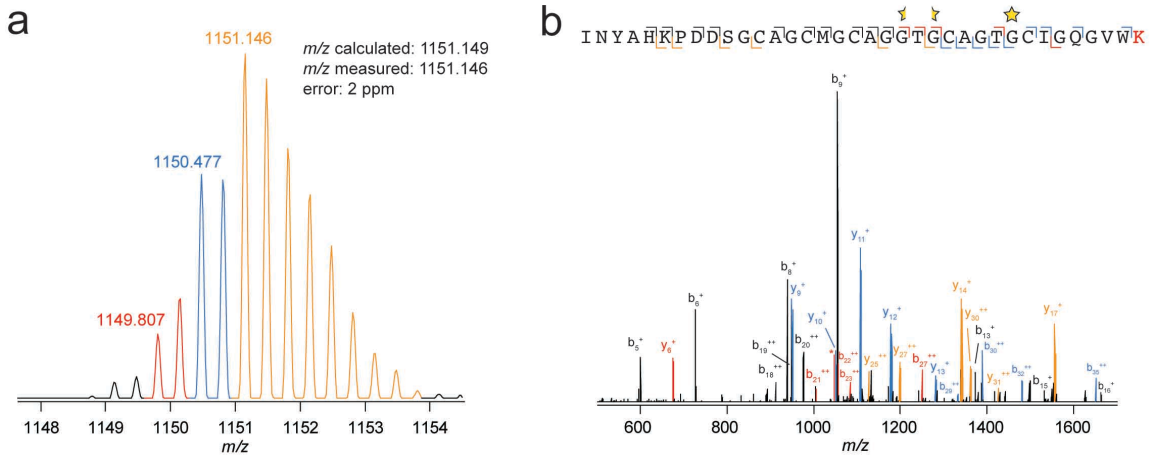

Figure S20. ^{18}O-labeling of plantazolicin. A MALDI-TOF spectrum demonstrating that AMPL can be utilized to selectively ^{18}O-label the TOMM natural product plantazolicin (Pzn; Figure S1) is displayed. As expected based on the structure of Pzn, exposure to acid in [^{18}O]-H_2O results in the incorporation of a single ^{18}O label (+20 Da) into Pzn due to the hydrolysis of the single methyloxazoline ring. The ratio between the ^{18}O- and ^{16}O-labeled hydrolysis species (*m/z* 1356 and 1354, respectively) is due to the presence of ~10% [^{16}O]-H_2O in the sample. All masses are for the 1+ charge state and the mass shift relative to the unmodified species (*m/z* 1336) is shown below the mass label.

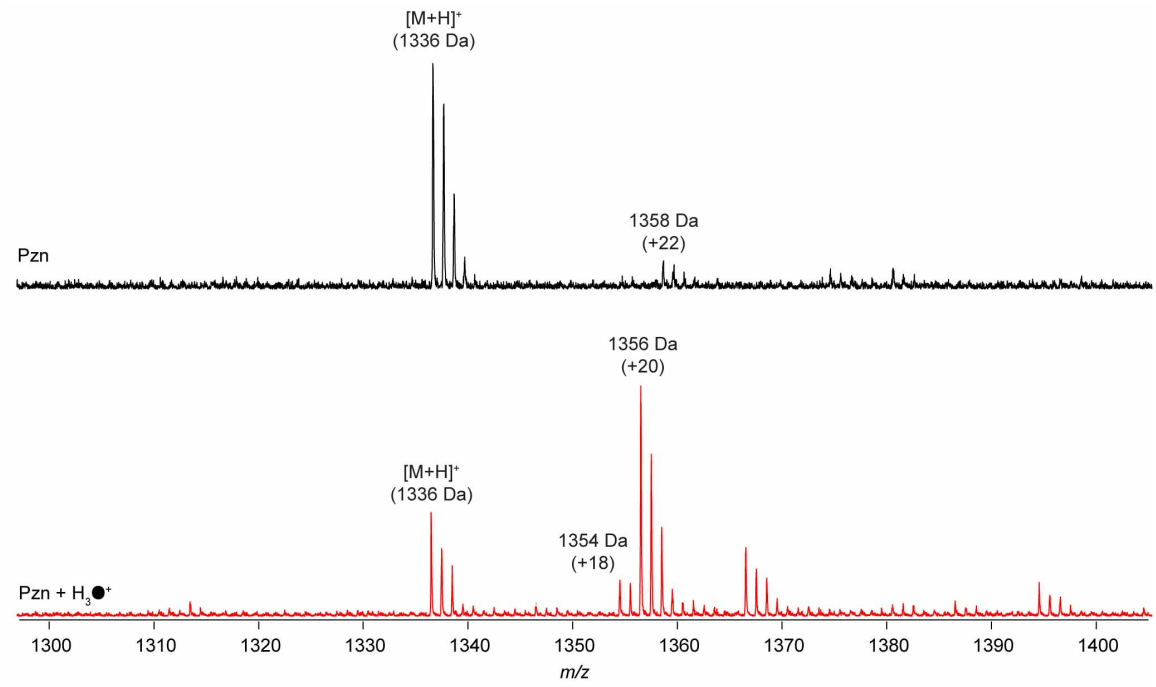

Figure S21. ^{18}O-labeling of ulithiacyclamide. A MALDI-TOF spectrum demonstrating that AMPL can be utilized to selectively ^{18}O-label the TOMM natural product ulithiacyclamide (Uli; Figure S1) is displayed. Based on the structure of Uli, exposure to acidified [^{18}O]-H_2O should result in the incorporation of two ^{18}O-labels (*m/z* 803.2). Although this peak is not detected, both the +Na (*m/z* 825.2) and +K (*m/z* 841.2) species are observed. All masses are for the 1+ charge state and the mass shift relative to the unmodified species (*m/z* 763.2) is shown below the mass label.

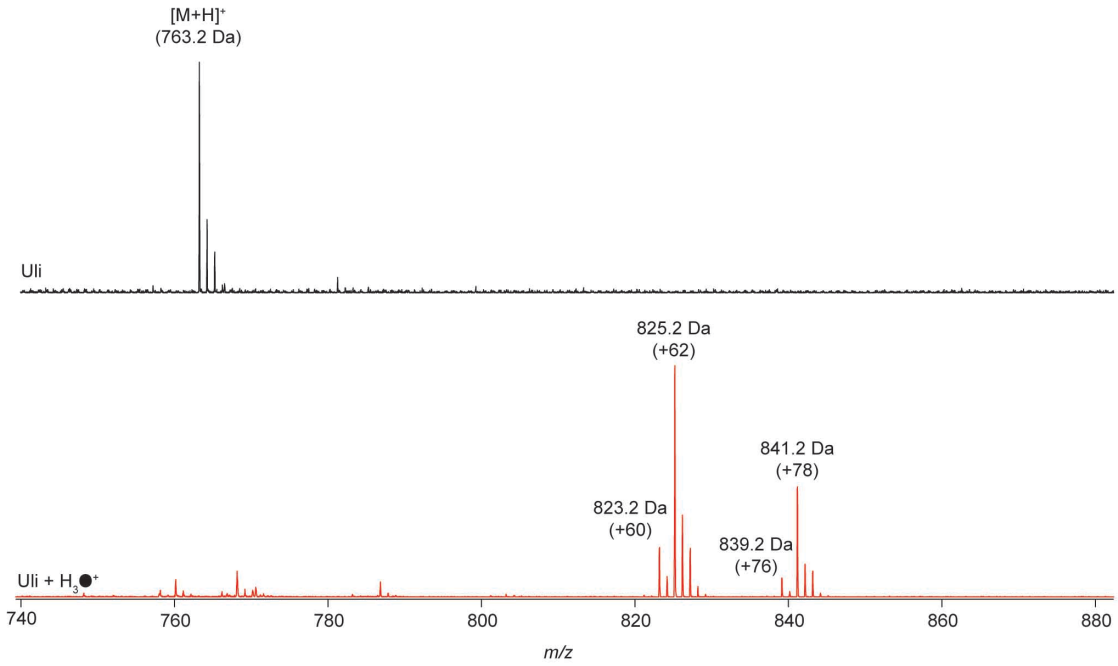

Figure S22. ^{18}O-labeling of lissoclinamide 4. A MALDI-TOF spectrum demonstrating that AMPL can be utilized to selectively ^{18}O-label the TOMM natural product lissoclinamide 4 (Lis; Figure S1) is displayed. While Lis contains two azoline heterocycles (a thiazoline and a methyloxazoline) a spectrum of the starting material (black) indicates that a majority of the species is hydrolyzed to begin with (+18 Da). As such, treatment with acidified [^{18}O]-H_2O is expected to generate a species containing both a ^{16}O and an ^{18}O label (*m/z* 780.2). Indeed this dual labeled product is obtained. All masses are for the 1+ charge state and the mass shift relative to the unmodified species (*m/z* 742.2) is shown below the mass label.

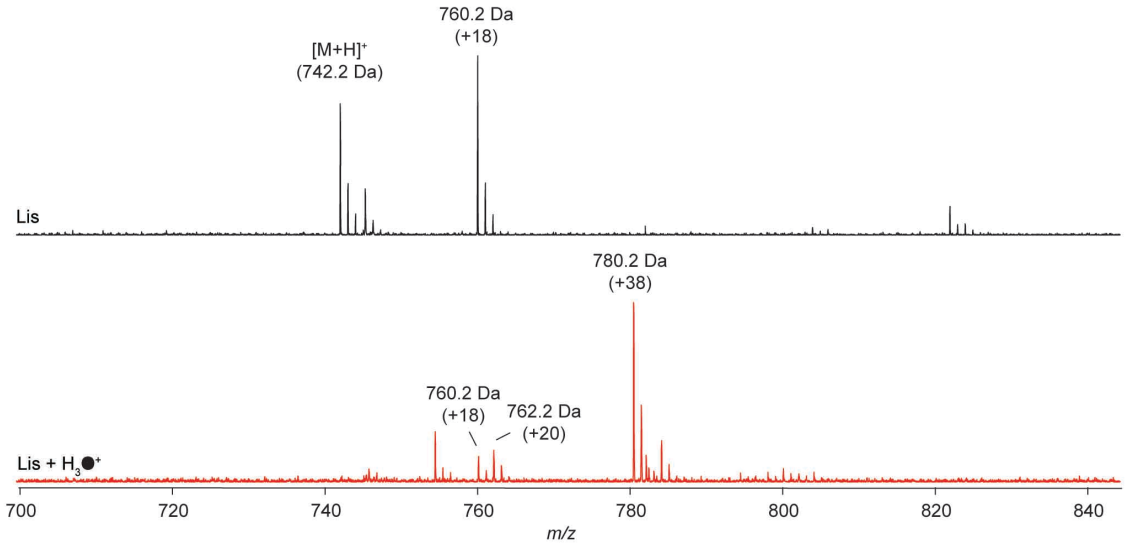

Supporting References

(1) Sievers, F.; Wilm, A.; Dineen, D.; Gibson, T. J.; Karplus, K.; Li, W.; Lopez, R.; McWilliam, H.; Remmert, M.; Soding, J.; Thompson, J. D.; Higgins, D. G. *Mol. Syst. Biol.* **2011**, *7*, 539.

(2) Dunbar, K. L.; Melby, J. O.; Mitchell, D. A. *Nat. Chem. Biol.* **2012**, *8*, 569.

(3) Sinha Roy, R.; Kelleher, N. L.; Milne, J. C.; Walsh, C. T. *Chem. Biol.* **1999**, *6*, 305.

(4) Melby, J. O.; Dunbar, K. L.; Trinh, N. Q.; Mitchell, D. A. *J. Am. Chem. Soc.* **2012**, *134*, 5309.

(5) Mitchell, D. A.; Lee, S. W.; Pence, M. A.; Markley, A. L.; Limm, J. D.; Nizet, V.; Dixon, J. E. *J. Biol. Chem.* **2009**, *284*, 13004.

(6) Lee, S. W.; Mitchell, D. A.; Markley, A. L.; Hensler, M. E.; Gonzalez, D.; Wohlrab, A.; Dorrestein, P. C.; Nizet, V.; Dixon, J. E. *Proc. Natl. Acad. Sci. U.S.A.* **2008**, *105*, 5879.

(7) Petritis, B. O.; Qian, W. J.; Camp, D. G., 2nd; Smith, R. D. *J. Proteome. Res.* **2009**, *8*, 2157.